JOURNAL OF CATALYSIS **105**, 405–415 (1987)

Steady-State and Isotopic Transient Kinetics of Benzene Hydrogenation on Nickel Catalysts

C. MIRODATOS,[1] J. A. DALMON, AND G. A. MARTIN

Institut de Recherches sur la Catalyse, Laboratoire Propre du CNRS conventionné à l'Université Claude Bernard Lyon I, 2 avenue Albert Einstein, 69626-Villeurbanne Cedex, France

Received September 30, 1985; revised November 28, 1985

By combining steady-state and isotopic transient experiments which provide both apparent and true kinetic parameters, we propose a modeling of the benzene hydrogenation reaction over nickel catalysts at low temperature (below 400 K). The metal surface is shown to be covered mainly with adsorbed hydrogen; only a very small fraction of the surface (about 1%) is covered with reacting intermediates. From the physically significant parameters thus determined, we arrive at the rate equation $r = k_0 e^{-E_0/RT}(1 - \theta_H)^X P_H P_B^{\varepsilon}$, where $E_0 = 33 \pm 4$ kJ/mol, θ_H-the surface coverage with hydrogen, $X = 4 \pm 1$, and P_H and P_B-partial pressures of hydrogen and benzene, respectively. The rate-limiting step can be described as a two-body process between (i) the active site, an ensemble of about four adjacent nickel atoms occupied by a chemisorbed benzene molecule, and (ii) a molecular hydrogen species. The concentration of the active ensembles is monitored by the hydrogen coverage, the latter being influenced little by the reservoir of loosely adsorbed benzene which coats and feeds the catalytic surface. © 1987 Academic Press, Inc.

INTRODUCTION

The hydrogenation of benzene on metals is widely used and studied as a test and model reaction in heterogeneous catalysis (*1*). However, there is still great controversy about its mechanism: basic considerations such as the nature of the active sites, the respective role of hydrogen and benzene adsorption, and the possible changes in mechanism over a wide temperature range remain open for discussion (*2–4*).

In a previous study (*5*), benzene hydrogenation over nickel-on-silica was examined from the viewpoint of structure sensitivity and copper alloying. For poorly dispersed samples obtained by reduction at high temperature, the decrease in intrinsic activity has been assigned to a strong metal–support interaction (SMSI). In the opposite case, i.e., for highly dispersed catalysts, a statistical approach based on the combined effects of particle size, surface coverage with adsorbed species, and active site dimension has been proposed to account for the observed changes in catalytic activity (*6*). Particularly, it was shown from the rate variations with copper alloying that the hydrogenation of benzene into cyclohexane requires the presence of about three adjacent nickel atoms (*5*). Concerning the coverage of the nickel surface, there are highly diverging opinions. Kehoe and Butt (*7*) concluded that there was saturation of the surface with benzene. However, the present authors favor a high coverage with adsorbed hydrogen, similar to the case for Pt/zeolite catalyst studied by Gallezot and Bergeret (*8*) using radial electron distribution method, where irreversibly adsorbed hydrogen was not displaced by benzene whatever its partial pressure.

To acquire key information concerning the occupancy of the catalytic surface during the reaction, in the absence of which mechanistic modeling is of dubious value, we have recently adapted the kinetic method of isotopic transients to benzene hydrogenation. The first results of this study (*9*) show that below 400 K the nickel

---

[1] To whom correspondence should be addressed.

0021-9517/87 $3.00

TABLE 1

Characteristics of Catalysts

No.	Precursor	Ni loading (wt%)	Reduction temperature (K)	Degree of reduction	Average particle size (nm)	BET area (m^2/g)
1	$Ni(OH)_2$	62	570	1.01	51.0[b]	10
2	$Ni(OH)_2/SiO_2$	4.5	800	0.95	2.5[a]	190
3	$Ni(OH)_2/SiO_2$	23	920	0.98	4.1[a] 6.4[b]	230
4	$Ni(OH)_2/SiO_2$	23	1200	1.0	14[b]	200
5	$Ni(OH_2)KNO_3/SiO_2$	23	920	1.0	6[a]	40

[a,b] Reduction at low (*a*) and high (*b*) heating rates (2 and 10 K/min, respectively).

surface is covered mainly with hydrogen and the concentration of activated benzene leading to cyclohexane is very low (less than 1% of the exposed metal atoms). A large reservoir of benzene forming a loosely adsorbed overlayer is also present on the whole surface of the catalyst.

The present paper aims at combining this transient approach with a kinetic study carried out in the steady-state regime in order to propose a possible mechanism for the hydrogenation of benzene into cyclohexane. It will apply mainly to the low-temperature range (below 400 K) since it has been shown previously that at higher temperature, side reactions, such as benzene hydrogenolysis into methane, coke deposition, and cyclohexene formation, and perhaps also some thermodynamic limitations do occur (*5*, *10*).

EXPERIMENTAL

Catalysts. Most of the nickel catalysts used in the present study were already described in previous papers (*5*, *6*, *11*). Their main characteristics (loading, average particle size determined by combined magnetic and electron microscope methods, temperature of reduction) are listed in Table 1. The precursors were prepared (i) for unsupported catalysts via decomposition of nickel nitrate hexammine into $Ni(OH)_2$ and (ii) for silica-based catalysts via impregnation of silica (Aerosil Degussa, 200 m^2/g) with a solution of nickel nitrate hexammine. These precursors were reduced under flowing dry hydrogen following temperature-programmed procedures. Some experiments were also performed on Ni–K/SiO_2 obtained by impregnating one of the $Ni(OH)_2/SiO_2$ precursors (that for sample 3) with KNO_3. It contained 2.7 wt% potassium.

Kinetic experiments. Both steady-state and transient experiments were carried out in flow systems with a fixed-bed reactor consisting of a quartz tube, the sample being held by quartz wool. Gases (H_2, He, or Ar) had an initial purity better than 99.99% and were further purified by a deoxo catalyst followed by zeolite traps. The partial pressure of benzene was varied by bubbling flowing reacting gases through liquid benzene. Light benzene (from Merck) was further purified by adding metallic sodium; deuterated benzene (99.6% D from CEA, France) was used without further treatment. Gas analyses were performed by gas chromatography with a flame-ionization detector for steady-state experiments.

The transient experiments were carried out by abruptly replacing the reacting gas mixture (i.e., $H_2 + C_6H_6$) with its labeled equivalent (i.e., $H_2 + C_6D_6$) without significant perturbations in flow and partial pressures. The transient changes in the isotopic composition at the reactor outlet were then analyzed by on-line mass spectrometry.

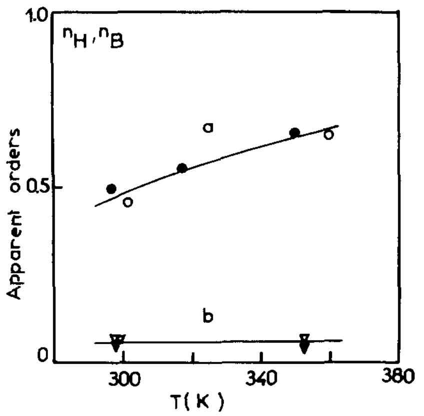

FIG. 1. Apparent orders with respect to hydrogen pressure, n_H (a), and benzene pressure, n_B (b) as a function of the temperature of reaction. Solid and open symbols: samples 1 and 3, respectively.

Experimental details as well as the fundamentals of the method are given in Ref. (9).

RESULTS

Apparent Kinetic Parameters for Benzene Hydrogenation in the Steady-State Regime

Figure 1 shows the influence of the reaction temperature on the orders with respect to hydrogen (n_H) and benzene (n_B). The kinetic parameters appear to be independent of the nature of the catalysts. Moreover, n_B appears to be temperature independent, lying between 0 and 0.1. The n_H values increase slightly as the temperature increases, in agreement with the data of van Meerten and Coenen (2). In Fig. 2, we observe that for sample 3, n_H decreases as the hydrogen pressure is increased. Similar results were obtained for the other samples studied. This kinetic feature reported here for benzene hydrogenation at low temperature is in good keeping with the observation reported in Ref. (2) at temperatures higher than 380 K. No significant change in the n_B value with hydrogen pressure is observed. The apparent activation energy measured from the Arrhenius plots below 400 K lies mainly around 50 kJ/mol, whether the catalyst is supported or not [see Fig. 3a and Ref. (5)]; however, this apparent activation energy tends to decrease with increasing temperature. We recall from Ref. (5) that at temperatures higher than 420 K, the slope of the Arrhenius plots starts to be negative and n_H tends to values as high as 3.

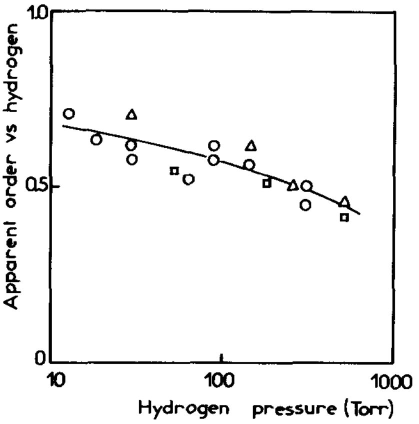

FIG. 2. Apparent order with respect to hydrogen pressure, n_H, as a function of the hydrogen pressure, measured at 300 K on sample 3 (circles, P_B = 40 Torr; squares, P_B = 1 Torr) and sample 1 (triangles, P_B = 2 Torr).

Transient Experiments

Figure 4 gives an example of transient curves obtained by replacing the reacting

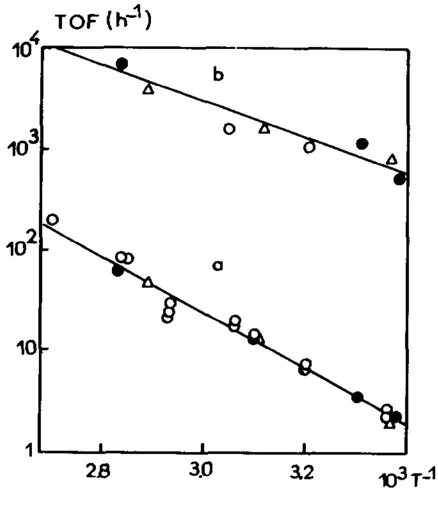

FIG. 3. Turnover frequency (TOF) expressed per exposed-surface atom (a) and per active site (b) as a function of the reciprocal temperature measured at P_H = 720 Torr and P_B = 40 Torr for sample 3 (open and solid circles, 3.6 and 36.0 mg of catalyst, respectively) and for sample 1 (triangles).

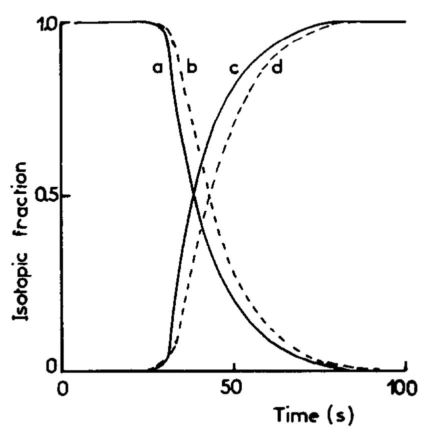

FIG. 4. Transient changes in the isotopic fraction of benzenes (a, C_6H_6; c, C_6D_6) and cyclohexanes (b, C_6H_{12}; d, $C_6H_6D_6$) on sample 3 at 300 K.

mixture C_6H_6/H_2 with its labeled equivalent C_6D_6/H_2. This method of tracing has been chosen to avoid the isotopic effects observed when H_2 is replaced by D_2 (*9*).

Reversible benzene adsorption during catalysis. From the time elapsed before light benzene is completely replaced by heavy benzene at the reactor outlet, i.e., from the integration under the benzene transient curves, one can obtain the amount of benzene that adsorbs reversibly on the catalytic surface under the reaction conditions [due corrections for chromatographic effects are required (*9*)]. These values are reported partially in Ref. (*9*) and are completed in Table 2 (columns 3 and 4) of the present paper. They indicate that more than one monolayer of loosely adsorbed benzene is present on the catalyst during the hydrogenation process at room temperature. This reservoir of benzene is shown to be very temperature sensitive. As a matter of fact, above 400 K, the transient curves of benzene are identical to the curve for a nonadsorbing gas such as helium or argon, which means that there is no more significant amount of benzene lying on the surface (let us emphasize that under these conditions, the catalytic activity is still very high).

Hydrogenation intermediates. From the delay observed between benzene and cyclohexane isotopic responses (again corrected for the chromatographic effect), we can evaluate directly the mean time it takes for a molecule of benzene to be transformed irreversibly into cyclohexane. In other words, we measure the mean lifetime of the precursors of cyclohexane on an active site (or on several sites if, for example, the overall process includes several steps with the migration of intermediate species onto the surface). The reciprocal of the lifetime then gives straightforwardly the mean turnover frequency (TOF) of *an active site*, without any assumption about the nature and concentration of these sites. Some val-

TABLE 2

Kinetic Data Obtained from Steady-State and Transient Experiments

Catalyst	Temperature of reaction (K)	Amount of reversible benzene (10^{-6} cm^3/cm^2_{cat})	Monolayer equivalent	Turnover frequency per active site (h^{-1})	Turnover frequency per exposed atom (h^{-1})
Ni/SiO_2 (sample 3)	297	13.6	1.48	1,084	2
	325	3.4	0.37	1,975	18
	351	0.7	0.08	6,827	82
	393			11,950	330
Unsupported nickel (sample 1)					
	295	15.9	1.75	1,031	2
	322	5.2	0.57	1,617	12
	345	0.9	0.10	4,182	48

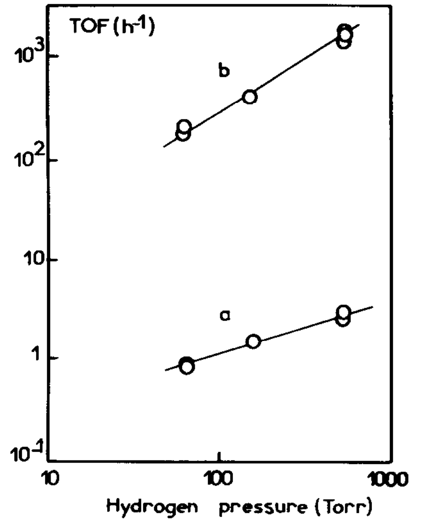

FIG. 5. Turnover frequency expressed per exposed-surface atom (a) and per active site (b) as a function of the hydrogen pressure for sample 1 at 300 K.

ues of this frequency are reported in Table 2 (column 5). These values can be compared with those for turnover frequency referred to *an exposed surface atom* as calculated from the overall rate of hydrogenation observed in the steady-state regime. The changes of these two TOFs with the temperature of reaction are illustrated by the Arrhenius plots in Figs. 3a and b. The apparent activation energies calculated from these plots are 50 kJ/mol (TOF/exposed surface atom) and 33 kJ/mol (TOF/active site). The orders in hydrogen pressure measured at room temperature in Fig. 5 are 0.52 (TOF/exposed surface atom) and 0.92 (TOF/active site). Changes of the two TOFs with benzene pressure are almost negligible.

Surface Coverage with Hydrogen

The titration of hydrogen chemisorbed on nickel catalysts in the absence of benzene has been extensively studied both volumetrically and magnetically. Complete adsorption isotherms for hydrogen are thus available, including coverages (θ_H) for the conditions of temperature and pressure used in the present hydrogenation study (*12*). The major question was then to determine to what extent the coadsorption of benzene (either the reversible or the reacting form) modifies the θ_H (P, T) laws worked out previously in the absence of benzene. Van Meerten *et al.* (*13*) have noted that the magnetic effect of hydrogen adsorption on a nickel surface precovered with benzene is nearly similar to the effect observed with a clean catalyst. Candy *et al.* (*14*) have estimated volumetrically that the amount of hydrogen chemisorbed on bare Raney nickel decreases by 12% if the surface is precovered with benzene. We have recently reached similar conclusions by titrating the hydrogen chemisorbed in the absence or in the presence of benzene under reaction conditions by deuterium after a controlled argon flush (*9*). Thus, it has been shown unambiguously that the hydrogen (or deuterium) coverages in the absence or in the presence of benzene were only slightly different. After having completed the results reported in Ref. (*9*), we will then consider further that under the temperature and pressure conditions investigated in the present kinetic study, the coverages with hydrogen in the presence of benzene are decreased by 5% in comparison with the coverages achieved in the absence of benzene. This gives θ_H values ranging from 0.65 to 0.80 under the reaction conditions.

Isotopic Distribution of Cyclohexanes

To obtain information about the mechanism of hydrogenation, experiments have been carried out under the steady-state regime by using the equimolecular mixture H_2–D_2 instead of pure H_2 or pure D_2. Let us assume that the secondary reaction $H_2 + D_2 \rightleftharpoons 2\,HD$ does not occur during the hydrogenation. For this ideal case, a mechanism of benzene hydrogenation via successive pairwise addition, namely

$$C_6H_6 + H_2 \rightarrow C_6H_8$$

$$C_6H_8 + H_2 \rightarrow C_6H_{10}$$

$$C_6H_{10} + H_2 \rightarrow C_6H_{12}$$

would give the first isotopic distribution of cyclohexane reported in Table 3, to the extent that the scrambling and isotopic effect are negligible (*9*). On the other hand, a mechanism by atomic addition, which would imply hydrogenation of the benzene molecule via dissociated hydrogen on the surface, would give the second isotopic distribution in Table 3. Unfortunately, for most of the hydrogenation conditions, the extent of the H_2–D_2 exchange reaction renders the two theoretical distributions of cyclohexanes very close [they are identical for the mixture $H_2/D_2/2HD$ (Table 3, third and fourth distributions)], which prevents us from distinguishing the two mechanistic pathways.

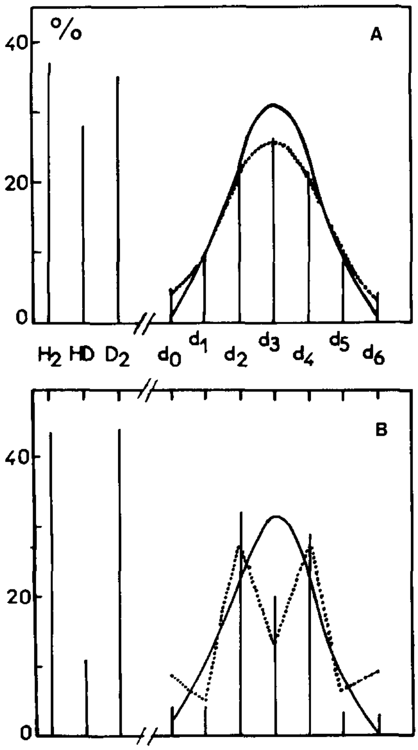

FIG. 6. Comparison between the experimental isotopic distributions of cyclohexane (bars) with $d_0 = C_6H_{12}$, $d_1 = C_6H_{11}D$, . . . , $d_6 = C_6H_6D_6$ and the theoretical distributions calculated by assuming stepwise (solid line) or pairwise (dotted line) addition of hydrogen, for two different isotopic distributions of hydrogen. (A) Sample 3 at 277 K, P_H = 10 Torr, P_B = 2 Torr. (B) Sample 5 at 353 K, P_H = 190 Torr, P_B = 40 Torr.

TABLE 3

Isotopic Distribution of Cyclohexanes Calculated for Different $H_2/D_2/HD$ Mixtures and According to Various Modes of Hydrogen Addition to Benzene

Hydrogen mixture (%)			Mode of hydrogen addition	Cyclohexane distribution (%)						
H_2	D_2	HD		d_0	d_1	d_2	d_3	d_4	d_5	d_6
50	50	0	Pairwise	12.5	0	37.5	0	37.5	0	12.5
			Atomic	1.5	9.4	23.4	31.2	23.4	9.4	1.5
25	25	50	Pairwise	1.5	9.4	23.4	31.2	23.4	9.4	1.5
			Atomic	1.5	9.4	23.4	31.2	23.4	9.4	1.5

Note. $d_0 = C_6H_{12}$, $d_1 = C_6H_{11}D$, . . . , $d_6 = C_6H_6D_6$.

By using extreme catalytic conditions, namely, low temperature, low hydrogen pressure, and less active catalysts (such as potassium-doped Ni/SiO_2, sample 5), we have nevertheless obtained some significantly distinguishable distributions. They are reported in Fig. 6. For the two cases, there is a rather marked similarity between the experimental distribution and the distribution calculated by assuming pairwise addition of hydrogen to the molecule of benzene. This is much at variance with the mechanisms already proposed which assume a sequence of hydrogen atom addition steps (*2*, *3*).

DISCUSSION

Steady-State Kinetic Data

If one considers (i) the surface of the working catalyst as being covered mainly with hydrogen as shown by titration under reaction conditions and (ii) the decrease in n_H, the partial order with respect to hydrogen pressure, when P_{H_2} increases (Fig. 2) or when the temperature of reaction decreases (Fig. 1), it may be deduced that the chemisorbed hydrogen plays, at least partially, an inhibiting role toward the rate of hydrogenation, although the overall order remains positive under the present reaction conditions. Let us now give a more quantitative treatment of this statement.

In a previous paper dealing with ethane hydrogenolysis on nickel (*12*), it had been

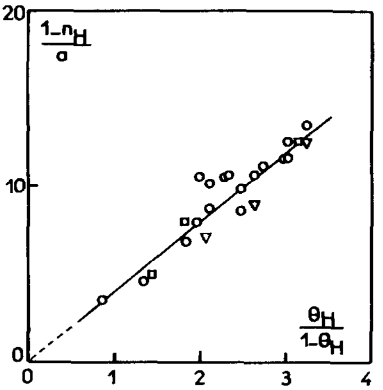

FIG. 7. Changes in the function $1 - n_H/a$ with the function $\theta_H/1 - \theta_H$ for samples 2 (triangles), 3 (circles), and 4 (squares).

shown that variations in n_H with temperature and pressure were quantitatively accounted for by the kinetic law

$$r = k(1 - \theta_H)^X. \qquad (1)$$

Let us recall briefly that this equation is mathematically equivalent to

$$n_H/a = -X\theta_H/(1 - \theta_H) \qquad (2)$$

where $a = (\delta \log \theta_H/\delta \log P_H)_T$. For the case of H_2 adsorption over the Ni/SiO_2 catalysts studied (sample 3), Freundlich isotherms were observed and a was straightforwardly deduced from the slope of the curves of log V vs log P. Then, by plotting n_H/a against $\theta_H/(1 - \theta_H)$ for ethane hydrogenolysis, a straight line with a slope $X = 15$ and an intercept at the origin was achieved.

No similar correlation was found for the present case of benzene hydrogenation. However, if one plots, $(1 - n_H)/a$ instead of n_H/a against $\theta_H/(1 - \theta_H)$, then a satisfying correlation is obtained giving a value for X of 4 ± 1, as depicted in Fig. 7. Such a correlation corresponds to the rate equation

$$r = kP_H(1 - \theta_H)^X \qquad (3)$$

with $X = 4 \pm 1$, which fully accounts for the experimental changes of n_H with T and P as shown in Figs. 1 and 2, the full lines being calculated from Eq. (3) as a reciprocal check. The term $(1 - \theta_H)^X$ could sense the inhibiting role of adsorbed hydrogen, yielding a negative partial order in hydrogen, although the overall order in hydrogen remains positive due to the term P_H in Eq. (3). This equation can be completed by including a term related to benzene pressure $P_B^{n_B}$ (nearly negligible since $n_B = 0.08$) and the true frequency and energy factors k_0 and $e^{-E_0/RT}$. This gives

$$r = k_0e^{-E_0/RT}(1 - \theta_H)^X P_H^1 P_B^{n_B} \qquad (4)$$

where $X = 4 \pm 1$ and $n_B = 0.08$.

As originally demonstrated by Temkin (*15*) and more recently applied by Martin (*12*) and by Frennet *et al.* (*16*), the apparent activation energy E_a results from the true activation energy E_0 modified by the activation energies related to the variations of coverage of the adsorbed species with temperature. For the present case, one obtains

$$E_a = E_0 + E_{\theta_H} + E_{\theta_B} \qquad (5)$$

where

$$E_{\theta_H} = -R(\delta \log(1 - \theta_H)^X/\delta(1/T))_{P_H,P_B}$$
$$E_{\theta_B} = -R(\delta \log P_B^{n_B}/\delta(1/T))_{P_H,P_B}.$$

As shown in Fig. 1, n_B does not vary significantly with T; so E_{θ_B} can be considered as negligible.

In Fig. 8, the Arrhenius transforms of the function $(1 - \theta_H)^X$ calculated from the variations of hydrogen coverage with temperature (see Surface Coverage with Hydrogen under Results) are plotted as dotted lines for $X = 1$ to 5. This gives as a mean value $E_{\theta_H} = 17 \pm 4$ kJ/mol for $X = 4 \pm 1$. E_0 can therefore be deduced from Eq. (5), taking $E_a = 50$ kJ/mol as a mean value in the range studied. This gives $E_0 = 33 \pm 4$ kJ/mol.

Considering the surface as covered mainly with hydrogen, the Temkin relation can also be expressed according to the equation

$$E_a = E_0 + (1 - n_H)Q_H \qquad (6)$$

$(1 - n_H)$ is used, as was done previously,

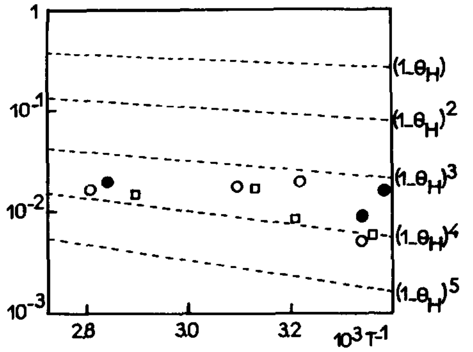

FIG. 8. Fraction of the active surface as a function of the reciprocal temperature for sample 1 (squares) and 3 (open and solid circles, 3.6 and 36.0 mg of catalyst, respectively). Dashed lines show the calculated function $(1 - \theta_H)^X$, where $X = 1$ to 5.

instead of n_H as the order related to chemisorbed hydrogen and Q_H is the isosteric heat of hydrogen adsorption for the reaction conditions. Figure 9 illustrates that the experimental changes of E_a versus n_H can be satisfactorily accounted for by Eq. (6) assuming $Q_H = 30$ kJ/mol. This latter value of the isosteric heat of hydrogen adsorption on nickel is very plausible for these conditions (low temperature, high hydrogen coverage) if one refers to the calorimetric works of Wedler and Bröcker (*17*) and of Prinsloo and Gravelle (*18*). Extrapolation to $n_H = 1$ in Fig. 9 leads to $E_0 = 34$ kJ/mol in good keeping with the previous determination of the true activation energy.

Knowing E_0, one can calculate the true frequency factor k_0 from Eq. (4), which gives $k_0 = 480$ molec/s/Ni$_S$/Torr H_2. This value is discussed in a later section.

Transient Kinetic Data

The reciprocal value of the mean lifetime of cyclohexane precursors has been shown to be equivalent to the turnover frequency pertaining to *one active site*. This provides a direct insight into the elementary step (or sequence of elementary steps) which controls the overall rate of the reaction. The Arrhenius transform of this reciprocal function will give by inference the true activation energy of the reaction. The value of 36 ± 4 kJ/mol which is obtained from Fig. 3b agrees perfectly with the E_0 value calculated previously from the steady-state kinetic data on the basis of the Temkin equations (5) and (6). Such a convergence between two totally independent methods for determining E_0 strengthens considerably both the steady-state and the transient kinetic approaches developed in the present study.

It has been shown in Table 2 that the values of the TOF/active site were reasonably independent of the sample weight, the nickel dispersion, and the nature of the support, which corroborates the general trend of benzene hydrogenation to be structure insensitive (*19*), at least for medium-size particles and catalysts in a non-SMSI state (*5*). It can therefore be inferred that an active site is not related to topologically identifiable surface atoms [such kinetic homogeneity of the active surface does not exclude, however, a crystallographic heterogeneity of the nickel particles, as discussed by van Meerten and Coenen in Ref. (*2*)]. On this basis, one can define the fraction of metallic surface that "works" in the reaction, or the fraction of active surface, F_{act}, as

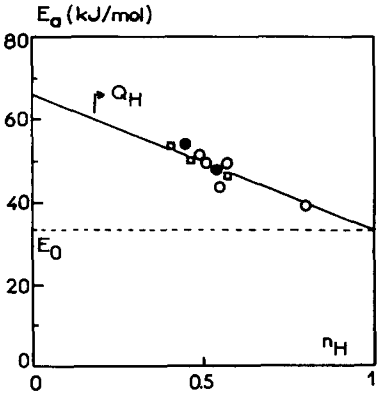

FIG. 9. Changes in the apparent activation energy (E_a) as a function of the apparent order versus hydrogen (n_H). The straight line obeys the equation $E_a = E_0 + (1 - n_H)Q_H$, where the intercept $E_0 = 33$ kJ/mol and the slope $Q_H = 30$ kJ/mol.

$$F_{act} = \frac{\text{number of active surface atoms}}{\text{total number of surface atoms}}. \quad (7)$$

Within the assumption that one site active in benzene hydrogenation requires N surface nickel atoms, which is in line with the idea of ensembles already developed for other reactions (*5, 6, 12, 16*), one obtains

$$F_{act} = \frac{(\text{TOF/exposed surface atom})}{1/N(\text{TOF/active site})} \quad (8)$$

Since the two TOFs are known from steady-state and transient experiments, respectively, this fraction can be straightforwardly calculated for given N values. We regarded it as of major interest to compare this fraction with the function $(1 - \theta_H)^X$. As a matter of fact, the latter expresses the statistical probability for an ensemble of X adjacent nickel atoms free from hydrogen to exist, owing to the surface occupancy by hydrogen (*6, 12, 16*), i.e., another way of defining the fraction of active surface. A unique and satisfying correspondence between the two functions is obtained if one takes $N = X = 4 \pm 1$ as depicted in Fig. 8. Such a statement strongly suggests that one should describe the active site for benzene hydrogenation as an ensemble of about four nickel surface atoms, the concentration being monitored by the H coverage. This is in good keeping with the value $N = 3 \pm 2$ assumed in the Ni–Cu alloy studies (*5*). This also underlines the physical meaning of the term $(1 - \theta_H)^X$, with $X = 4 \pm 1$, in the rate equation (4) obtained from steady-state measurements.

The number of nickel atoms composing the active site may also be compared with that deduced from volumetric measurements by Candy *et al.* (*14*): the consumption of hydrogen in contact with a nickel surface precovered with hydrogen indicates that the benzene that is hydrogenated is bonded to $N = 1.6$ nickel atoms. However, these authors have assumed that saturation in hydrogen coverage is achieved at room temperature under 10 Torr. We think that a θ_H value of 0.6 would better correspond to the pertaining temperature and pressure conditions. This would give $N = 1.6/0.6 = 2.7$, which is now consistent with the value determined in the present paper.

Besides this function of diluent of the active surface by inhibition of adspecies, hydrogen obviously also acts as a reactant in the hydrogenation process. This specific function is attested by the true order $(n_H)_0 = 0.9 \pm 0.1$ determined from the variation of the TOF/active site against the pressure of H_2 (Fig. 5b). This order, near unity, is quite consistent with the term P_{H_2} in the rate equation (*4*) which then reflects by itself this reacting function of hydrogen.

Mechanism of Benzene Hydrogenation

From all these statements and the physical meaning of each parameter of the rate equation (4)

$$r = k_0 e^{-E_0/RT}(1 - \theta_H)^4 P_H^1 P_B^{\varepsilon}$$

the rate-limiting step of the benzene hydrogenation on nickel at low temperature may be described as a two-body process between (i) an ensemble of about 4 Ni atoms occupied by a chemisorbed molecule of benzene (this benzene would be supplied by the loosely adsorbed reservoir that coats the whole surface of the catalyst, the chemisorption occurring as soon as suitable sites appear on the Ni surface covered mainly with hydrogen) and (ii) a molecular species of hydrogen, probably coming from the gas phase since its concentration is related to P_{H_2}.

This picture does not necessarily imply an Eley–Rideal mechanism as proposed in Refs. (*7, 20*). Equation (*4*) means only that the rate-determining step of the whole process is determined by the probability of a collision between a gaseous H_2 molecule and the surface complex. For instance, this molecular species of hydrogen could first adsorb near the reactive benzene by forming an adsorbed complex before the proper hydrogenation of the aromatic ring which would then be restricted to the reaction of two adsorbed species.

A rough estimation of the sticking coefficient of such a two-body step may be obtained from the ratio of the true frequency factor, k_0, to the frequency of collision of H_2 molecules with the surface as calculated from the kinetic theory of gases. This gives

$$\frac{480 \text{ molec/s/Ni}_S\text{/Torr H}_2}{5 \times 10^5 \text{ collisions/s/Ni}_S\text{/Torr H}_2} = 10^{-3} \text{ molec/collision.}$$

Such a value does not seem unreasonable because there is uncertainty in the E_0 determination and also because a molecule of H_2 colliding with the surface would probably have a large tendency to desorb or to dissociate and to participate in the inhibiting coverage of nickel rather than to react with the chemisorbed benzene.

Accounting for the above description of the rate-limiting step, which still remains far from being completely elucidated, and accounting also for the tendency for hydrogen to be added according to a sequence of pairwise addition steps (see Results), we tentatively propose the events shown in Scheme 1 to describe the overall reaction.

1	$H_{2_{gas}} + 2Ni_S \rightleftharpoons 2H_{ads}$	Fast, monitors the concentration of active sites
2	$C_6H_{6_{gas}} \rightleftharpoons C_6H_{6_{rev}}$	Fast, forms a reservoir of loosely adsorbed benzene
3	$C_6H_{6_{rev}} + 4Ni_S \rightarrow C_6H_{6_{irrev}}$	Fast but regulated by the concentration of ensembles $4Ni_S$, saturates the free active sites
4	$C_6H_{6_{irrev}} + H_2 \rightarrow C_6H_{8_{ad}}$	Slow, rate-limiting step with known k_0 and E_0[a]
5	$C_6H_{8_{ad}} + H_2 \rightarrow C_6H_{10_{ad}}$	Irreversible and fast reactions since no intermediate products are detected and no back-scrambling is observed from cyclohexane to benzene under exchange conditions (9)
6	$C_6H_{10_{ad}} + H_2 \rightarrow C_6H_{12_{ad}}$	
7	$C_6H_{12_{ad}} \rightarrow C_6H_{12_{rev}} + 4Ni_S$	
8	$C_6H_{12_{rev}} \rightleftharpoons C_6H_{12_{gas}}$	Fast, weak adsorption, similar to Reaction 2 with benzene; accounts for the chromatographic effects detected for cyclohexane (9)

[a] This step, which does not imply an Eley–Rideal mechanism, could be an oversimplification of more complex elementary steps, following, for instance, as discussed above,

$$C_6H_{6_{irrev}} + H_2 \xrightarrow{\text{rds}} [C_6H_6, H_2]_{ad} \xrightarrow{\text{fast}} C_6H_{8_{ad}}$$

SCHEME 1. Overall reaction of benzene hydrogenation.

This overall scheme of hydrogenation does not report the side reactions of benzene and cyclohexane exchange which proceed very probably via totally different pathways. These reactions display different kinetic orders and activation energies and yield mainly a stepwise exchange (*21*) which fundamentally differs from pairwise addition of hydrogen. Moreover, they could imply a σ-type adsorption of benzene (*22*) rather than a π-type adsorption which is generally postulated for benzene hydrogenation and which corresponds better to the site geometry determined in the present study.

Although the above scheme accounts satisfactorily for the hydrogenation at low temperature, it is probably no longer valid at high temperature. As a matter of fact, besides the changes in kinetic parameters and the breakthrough of other side reactions such as benzene cracking, the reservoir of benzene formed from step 2 no longer exists at $T > 400$ K. Moreover, the desorption of cyclohexene (*5*) clearly indicates major changes in the relative sequence of rate constants of steps 5 to 8. All these observations render questionable in our opinion any attempt to describe the reaction of benzene hydrogenation by a sole mechanism over a large range of temperature and pressure conditions. Further studies are in progress to propose a kinetic explanation for the high-temperature behavior.

CONCLUSION

From the viewpoint of methodology, a main feature of the present study has been to show that a combined kinetic approach via steady-state and transient experiments is very fruitful. Although the formalism based on the Temkin relation and the concept of site/ensemble itself allows the proposal of an overall rate equation, physically meaningful, the isotopic transient kinetics provide direct and quantitative data related to the rate-determining step, and they are therefore assumed to give the true parameters of the reaction.

For the mechanism of benzene hydrogenation at mild temperature, this combined study suggests that the rate-limiting step could be a two-body process between a benzene molecule irreversibly adsorbed on about four nickel atoms and a molecular hydrogen species. Although the whole metallic surface is probably potentially active for the benzene hydrogenation, in good keeping with its structure insensitivity, only a very small fraction of the surface atoms are actually doing the work (less than 1% at room temperature). This is the result of the dynamic and statistical occupation of a large part of the surface by hydrogen, this coverage being influenced little by a coating of loosely and reversibly adsorbed benzene. In that sense, the active site is shown in the present study not to be related to certain special atoms but to depend on a statistical occupation of the surface by adsorbates.

REFERENCES

1. Moyes, R. B., and Wells, P. B., *in* "Advances in Catalysis" (D. D. Eley, H. Pines, and P. B. Weisz, Eds.), Vol 23, p. 121. Academic Press, New York, 1973.
2. van Meerten, R. Z. C., and Coenen, J. W. E., *J. Catal.* **37,** 37 (1975); **46,** 13 (1977).
3. Franco, H. A., and Phillips, M. J., *J. Catal.* **63,** 346 (1980).
4. Parmaliana, A., El Sawi, M., Fedele, U., Giordano, G., Frusteri, F., Mento, G., and Giordano, N., *Appl. Catal.* **12,** 49 (1984).
5. Martin, G. A., and Dalmon, J. A., *J. Catal.* **75,** 233 (1982).
6. Martin, G. A., Dalmon, J. A., and Mirodatos, C., *in* "Proceedings, International Congress on Catalysis, 8th (Berlin, 1984)," Vol IV, p. 371. Verlag Chemie, Weinheim, 1984.
7. Kehoe, J. P. G., and Butt, J. B., *J. Appl. Chem. Biotechnol.* **22,** 23 (1972).
8. Gallezot, P., and Bergeret, G., *J. Catal.* **72,** 294 (1981).
9. Mirodatos, C., *J. Phys. Chem.* **90,** 681 (1986).
10. Van Barneveld, W. A. A., and Ponec, V. *Rec. Trav. Chim.* **93,** 243 (1974).
11. Primet, M., Dalmon, J. A., and Martin, G. A., *J. Catal.* **46,** 25 (1977).
12. Martin, G. A., *J. Catal.* **60,** 345 (1979).
13. van Meerten, R. Z. C., de Graaf, T. F. M., and Coenen, J. W. E., *J. Catal.* **46,** 1 (1977).
14. Candy, J. P., Fouilloux, P., and Imelik, B., *Nouv. J. Chim.* **2,** 45 (1977).
15. Temkin, M., *Acta Physicochim. URSS* **2,** 313 (1935).
16. Frennet, A., Lienard, G., Crucq, A., and Degols, L., *J. Catal.* **53,** 150 (1978).
17. Wedler, G., and Bröcker, F. J., *Surf. Sci.* **26,** 389 (1971).
18. Prinsloo, J. J. and Gravelle, P. C., *J. Chem. Soc. Faraday Trans. I* **76,** 2221 (1980).
19. Dalmai-Imelik, G., and Massardier, J., *in* "Proceedings, International Congress on Catalysis, 6th (London 1976)," p. 90. Chemical Society, London, 1977.
20. Parmaliana, A., El Sawi, M., Mento, G., Fedele, V., and Giordano, N., *Appl. Catal.* **7,** 221 (1983).
21. van Meerten, R. Z. C., Morales, A., Barbier, J., and Maurel, R., *J. Catal.* **58,** 43 (1979).
22. Moyes, R. B., Baron, K., and Squire, R. C., *J. Catal.* **22,** 33 (1970).